JOURNAL OF Materials CHEMISTRY

Crystal structure, thermal behaviour and zeolitic properties of $Cd_2Zr(C_2O_4)_4\cdot(4+n)H_2O$

Erwann Jeanneau, Nathalie Audebrand, Jean-Paul Auffrédic and Daniel Louër*

Laboratoire de Chimie du Solide et Inorganique Moléculaire, UMR CNRS 6511, Institut de Chimie, Université de Rennes I, Avenue du Général Leclerc, 35042 Rennes cedex, France. E-mail: Daniel.Louer@univ-rennes1.fr

Received 25th April 2001, Accepted 22nd June 2001
First published as an Advance Article on the web 13th August 2001

The crystal structure of the new mixed oxalate $Cd_2Zr(C_2O_4)_4\cdot(4+n)H_2O$ has been solved from single-crystal diffraction data. A powder diffraction study has shown that the compound crystallises with orthorhombic symmetry. The structure has been solved in space group *Imm*2 ($Z=2$). The structure is built from chains of eight-fold coordinated cadmium atoms linked to eight-fold coordinated zirconium atoms through bidentate oxalate groups. The structure has an open framework exhibiting tunnels with square and ellipsoidal cross-sections, filled with 'zeolitic' water molecules. The initial dehydration process is reversible and occurs with an anisotropic elastic behaviour of the structure framework. The enthalpy and entropy of the dehydration reaction have been determined. They are $\Delta_r H=49(2)$ kJ mol^{-1} and $\Delta_r S=123(3)$ J K^{-1} mol^{-1} for the initial dehydration stage, which is related to the departure of 'zeolitic' water molecules, and $\Delta_r H=80(1)$ kJ mol^{-1}and $\Delta_r S=141(2)$ J K^{-1} mol^{-1} for the second stage related to the departure of bonded water molecules. The complete decomposition scheme into cubic zirconium oxide and cadmium oxide is reported from a thermal analysis study, including temperature-dependent powder diffraction.

Introduction

In recent studies, new mixed oxalates involving two eight-fold coordinated metals, *e.g.* $YK(C_2O_4)_2\cdot 4H_2O$[1] and $Pb_2Zr(C_2O_4)_4\cdot nH_2O$ ($3<n<9$),[2] have been reported. Although the two three-dimensional structure frameworks are different, interesting reversible dynamic properties arising from 'zeolitic' water molecules, located in the cavities of the open structures, have been identified and thoroughly characterised. The presence of cavities in the crystal structure of a number of oxalates has been reported long ago[3–5] and zeolitic properties due to weakly bonded water molecules located in these voids have been discussed.[1,2,6] In the case of the two previous mixed oxalates, the structure framework includes eight-fold coordinated polyhedra for the two metals in the chemical formula. This feature suggests that such eight-fold coordination polyhedra could be simple basic structural units to be considered for the synthesis of new related compounds, similarly to the role played by building units in conceiving new materials.[7] Zirconium is frequently eight-fold coordinated. Lead, well known for having flexible coordination polyhedra, can be found with an eight-fold coordination, as for instance in $Pb_2Zr(C_2O_4)_4\cdot nH_2O$.[2] Cadmium, which is also characterised by a certain flexibility of its coordination polyhedra, could be considered as a possible candidate in such syntheses. It was then anticipated that chemical combinations between zirconium and cadmium could occur in the oxalate family. This idea has been successfully applied, as shown here by the synthesis of a new mixed cadmium zirconium oxalate with interesting zeolitic properties. The present study deals with the crystal structure determination and the thermal behaviour of $Cd_2Zr(C_2O_4)_4\cdot nH_2O$. Moreover, due to the dynamic behaviour of water molecules, a careful investigation of the thermodynamical equilibrium between the precursor and water vapour is reported.

Synthesis

Crystals of mixed cadmium zirconium oxalate were obtained by slow evaporation of cadmium nitrate, zirconium oxynitrate and oxalic acid solution. 0.50 g of cadmium nitrate $Cd(NO_3)_2\cdot 4H_2O$ (Merck) and 0.37 g of zirconium oxynitrate $ZrO(NO_3)_2\cdot xH_2O$ from Alpha [whose correct formula is in fact $Zr(OH)_2(NO_3)_2\cdot(1+x)H_2O$][8] were dissolved in 20 mL of water. A white precipitate was formed from the titration of this solution by a solution of oxalic acid (0.1 mol L^{-1}) in excess. The solution was heated to 35 °C under constant stirring until the precipitate dissolved. The evaporation of the solution at this temperature produced a microcrystalline powder of the new cadmium zirconium oxalate. Moreover, many attempts to obtain larger crystals resulted only in the formation of tiny crystals. From a slower evaporation at room temperature, small bipyramidal transparent crystals of average size 20 μm were found, after a few hours, agglomerated and floating at the upper surface of the solution. The crystals were washed with water and ethanol and, then, dried under air. This preparation was found to be sensitive to some parameters, such as temperature and pH of the solution. Indeed, it was sometimes necessary to heat the solution up to 80 °C in order to dissolve the white precipitate, while in other cases the dissolution happened at room temperature. Nevertheless, the temperature at which the dissolution occurred did not seem to have any influence on the formation of the mixed cadmium zirconium oxalate. The chemical formula was derived from energy dispersive spectrometry (ratio Cd/Zr: 2) and the determination of the crystal structure reported here, which corresponds to the formula $Cd_2Zr(C_2O_4)_4\cdot 6.3H_2O$. It was confirmed by manganimetric titration of the oxalate content (mean observed value: 3.8). As shown by the thermal study described hereafter, the water content of the compound depends upon the water-vapour pressure in room air. The image made by means of a

DOI: 10.1039/b103711k

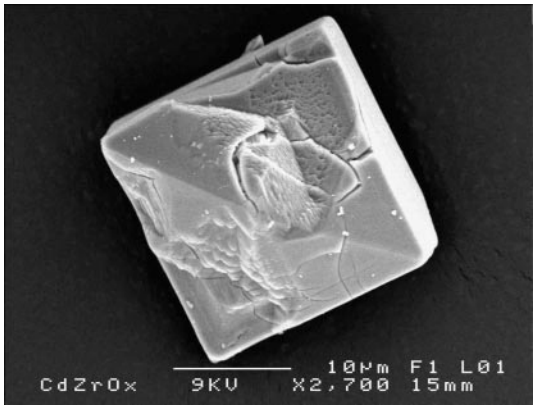

Fig. 1 Scanning electron microscope image of a bipyramidal-shaped $Cd_2Zr(C_2O_4)_4{\cdot}(4+n)H_2O$ crystal, showing the small size of the crystal and cracks due to the sensitivity towards the electron beam.

JEOL JSM-6301 F scanning electron microscope (Fig. 1) shows a typical bipyramidal-shaped crystal. Cracks in the crystal, due to the electron beam impact, can be seen on the figure. They demonstrate the high sensitivity of the product towards heat.

Experimental

Collection of X-ray powder diffraction data

X-Ray powder diffraction data were obtained with a Siemens D500 diffractometer with the parafocusing Bragg–Brentano geometry, using monochromatic Cu Kα_1 radiation (λ = 1.5406 Å) selected with an incident beam curved-crystal germanium monochromator.[9] The pattern was recorded under air over the angular range 9–80° (2θ) with a step length of 0.02° (2θ) and a counting time of 56 s step^{-1}. Additional powder diffraction data were collected *in situ* under constant total water-vapour pressure of 10 Torr generated as described hereafter, at different temperatures, with a Bruker AXS D5005 powder diffractometer (Cu Kα_1,α_2), equipped with an Anton Paar HTK1200 oven. For pattern indexing, the extraction of the peak positions was carried out with the Socabim program PROFILE, which is a part of the DIFFRACT-AT software package supplied by Bruker AXS. Pattern indexing was performed with the program DICVOL91.[10] Full-pattern matching was carried out with FULLPROF,[11] available in the software package WINPLOTR.[12]

Temperature-dependent X-ray diffraction (TDXD) was performed under dynamic air with a powder diffractometer combining the curved-position-sensitive (PSD) from INEL (CPS 120) and a high-temperature attachment from Rigaku. The detector was used in a semi-focusing arrangement by reflection (Cu Kα_1 radiation) as described elsewhere.[13]

Single-crystal data collection

A small crystal with linear dimensions lower than 40 µm was mounted on a four-circle Nonius Kappa CCD diffractometer, using Mo Kα radiation (λ = 0.71073 Å) and equipped with a CCD area detector. It was initially thought that the small size of the crystal would be partly compensated by fast data collection. In fact, the diffracting power was low and the total data collection exposure time required was 15 h. The experiment was carried out in the resolution range 20.00–0.71 Å with a crystal-to-detector distance of 25 mm. Intensities were collected by means of the program COLLECT[14] from 208 frames with a step rotation angle of 2° for the ω angle. Due to the small size of the crystal, each frame was obtained with a total exposure time of 300 seconds. Reflection indexing, Lorentz–polarisation correction, peak integration and background determination were carried out with the program DENZO.[15] Frame scaling and unit-cell parameters refinement were made with the program SCALEPACK,[15] on the basis of 2975 reflections in the θ range 1.02–30.03°. A cell search was carried out at the end of the experiment to confirm the stability of the crystal during data collection. Numerical absorption correction was performed by modelling the crystal faces using NUMABS.[16] However, due to the low absorption correction (T_{min} = 0.886, T_{max} = 0.901), the corrected data set did not improve the structure refinement. Crystallographic data and details on data collection are listed in Table 1. Structure drawings were carried out with Diamond 2.1c, supplied by Crystal Impact (Bonn, Germany).

CCDC reference number 165872.

See http://www.rsc.org/suppdata/jm/b1/b103711k/ for crystallographic data in CIF or other electronic format.

Thermal analysis

Thermogravimetric analyses (TG) were carried out either with a Rigaku thermoflex instrument for runs under air or a MacBain type thermobalance for runs under selected water-vapour pressures $P(H_2O)$ in the range 2–27 Torr. To generate this water vapour pressure, the thermobalance, connected to a bulb containing a sulfuric acid solution, was evacuated and then isolated from the vacuum pump. Different values of $P(H_2O)$ were obtained by changing the temperature and the concentration of the sulfuric acid solution. The values of $P(H_2O)$ were calculated from tables edited by Boll.[17] The powdered samples were spread evenly in large platinum crucibles to avoid mass effects.

Results

X-Ray powder diffraction study

As explained above the mixed cadmium zirconium oxalate was first obtained in a microcrystalline form and later as very small crystals. Initially, it was intended to proceed to the structure analysis from powder diffraction data, according to the procedure used in the studies of $YK(C_2O_4)_2{\cdot}4H_2O$[1] and

Table 1 Crystallographic data and structure refinement parameters for $Cd_2Zr(C_2O_4)_4{\cdot}6.3H_2O$

Empirical formula	$Cd_2ZrC_8O_{22.3}H_{12.6}$
Crystal system	Orthorhombic
Space group	*Imm*2 (no. 44)
Crystal size/mm	0.035 × 0.038 × 0.035
a/Å	11.2089(7)
b/Å	11.2083(6)
c/Å	8.4747(5)
V/Å^3	1064.7(1)
Z	2
Formula weight/g mol^{-1}	782.15
ρ_{calc}/g cm^{-3}	1.48
λ(Mo Kα)/Å	0.71073
θ range/°	1.02–30.03
Index ranges	$-15 \leqslant h \leqslant 15$, $-15 \leqslant k \leqslant 15$, $-11 \leqslant l \leqslant 11$
Unique data	1573
Observed data ($I > 4\sigma(I)$)	1114
R_1 ($I > 2\sigma(I)$)	0.068
R_1 (All)	0.101
wR_2 ($I > 2\sigma(I)$)	0.192
wR_2 (All)	0.172
Refinement method	Full-matrix least-squares on $\|F^2\|$
Goodness of fit	1.09
No. of variables	100
No. of constraints	4
Largest difference map peak and hole/e Å^{-3}	1.538 and −1.745

$Pb_2Zr(C_2O_4)_4{\cdot}nH_2O$.[2] Nevertheless, two major difficulties were encountered in both data collection and pattern indexing. Indeed, the samples were highly sensitive to ambient water-vapour pressure and slight temperature fluctuations, as seen from significant diffraction line shifts during data collection. For instance, it was noted that one of the three strongest lines at low angles, with a non-zero l index, could shift by 0.06° (2θ) in two data sets collected at a few hours interval. This is an indication that the cell dimensions could not be kept constant over the two days required to collect high resolution powder diffraction data. This effect is obviously related to changes in the water content in the sample with fluctuations of ambient water-vapour pressure and temperature. This feature is discussed in detail below.

In addition to the cumbersome effect of line shifts during data collection on pattern indexing, it was also noted, from data collected over a short time, that the indexing solution was somehow ambiguous. Indeed, due to the presence of slightly broadened diffraction lines, the suggested solutions were either a tetragonal cell or an orthorhombic one, whose esd's on dimensions could include the tetragonal parameters. This crystal symmetry problem was solved from data collected from a better crystallised sample. Fig. 2 shows the diffraction lines indexed as (400) and (040), from the data collected with monochromatic X-rays, demonstrating definitely the orthorhombic symmetry of the compound. To obtain precise parameters from peak positions stable during the experiment, powder data were collected with Cu $K\alpha_1,\alpha_2$ at 30 °C, under a total water-vapour pressure of 10 Torr. The pattern was indexed from DICVOL91 with an orthorhombic solution [$M_{20}=23$, $F_{20}=36(0.0118,47)$]. The cell parameters were refined from the full-pattern matching option available in FULLPROF, *i.e.* $a=11.2317(5)$ Å, $b=11.1777(6)$ Å and $c=8.4671(4)$ Å, $V=1063.0$ Å^3. The powder data have been submitted to the ICDD[18] for possible inclusion in the Powder Diffraction File. To ascertain that no tetragonal cell was obtained with increasing temperatures, an experiment was carried out as a function of temperature at a constant total water-vapour pressure of 10 Torr. Fig. 3 shows the decrease with temperature of the orthorhombic cell parameters. There is a decrease up to 80 °C of 0.7%, 0.8% and 1.3% for a, b and c, respectively. At temperatures greater than 80 °C, the unit cell parameters remain quasi-constant. This result contrasts with the behaviour of the yttrium potassium oxalate,[1] for which cell dimension changes occurred only from ~45 °C under ambient atmosphere, making easier the handling of the sample for X-ray powder diffraction at room temperature.

Due to the difficulties in having a stable powder material over time, it was decided to investigate the possibility of collecting diffraction data from single crystals, even given their tiny size.

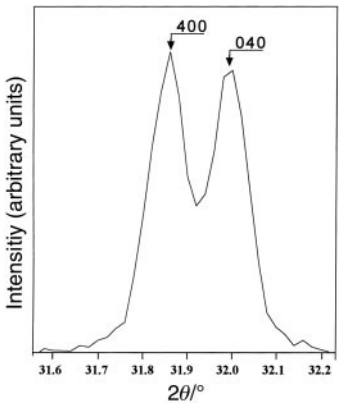

Fig. 2 Part of the powder diffraction pattern of $Cd_2Zr(C_2O_4)_4{\cdot}(4+n)H_2O$ showing the splitting of the 400 and 040 diffraction lines (Cu $K\alpha_1$ radiation), according to orthorhombic symmetry.

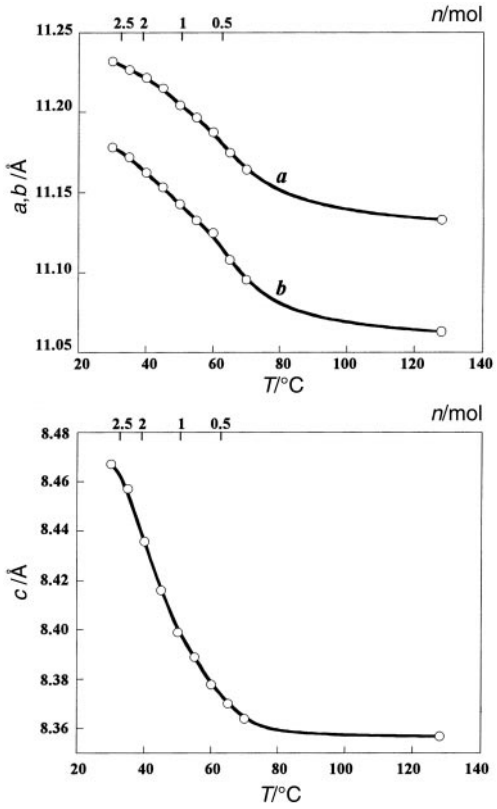

Fig. 3 Plot of the orthorhombic cell parameters as a function of temperature and water molecule content n, under a total water-vapour pressure of 10 Torr.

Structure solution from single-crystal data

Single-crystal diffraction data suggested again both a tetragonal solution and an orthorhombic cell with similar a and b parameters. However, attempts to solve the structure in the tetragonal system failed. Consequently, the orthorhombic symmetry was selected according to the results of the powder diffraction study. The refined cell parameters (Table 1) are consistent with those found from the indexing of the powder pattern data. The structure was solved in the space group *Imm*2 (systematic absence of hkl reflections with $h+k+l=2n+1$) by direct methods and the Patterson function using SIR97[19] and SHELXS97,[20] from which the heavy atoms were located. The remaining non H-atoms were located from successive Fourier map analyses using SHELXL97.[21] The last cycles of the refinement included atomic coordinates, anisotropic displacement parameters for all atoms, except oxygen atoms from water molecules, and occupancy factors of the oxygen atoms from the water molecules located inside the channels. Because of some instabilities during the refinement of one of the oxalate groups, probably due to the sensitivity of the 'elastic' structure framework towards water-vapour pressure variations over the 15 h data collection time, soft constraints were applied to the distances C2–O21, C2–O22 [1.25(2) Å] and C1–C2 [1.55(2) Å] within this oxalate group. Finally, the structure refinement agreed with the chemical formula $Cd_2Zr(C_2O_4)_4{\cdot}6.3H_2O$. The final atomic coordinates together with their equivalent isotropic displacement parameters are listed in Table 2. Selected bond distances and angles are reported in Table 3.

Description of the structure

The three-dimensional crystal structure of $Cd_2Zr(C_2O_4)_4{\cdot}6.3H_2O$ is built from eight-fold cadmium and zirconium polyhedra linked by oxalate groups. As shown in Fig. 4, the structure can be described by chains of CdO_8 polyhedra running along the c axis. These chains are formed by

Table 2 Positional and equivalent isotropic atomic displacement parameters with their standard deviations for $Cd_2Zr(C_2O_4)_4\cdot 6.3H_2O$. $U_{eq}=(1/3)\sum_i\sum_j U_{ij}a_i^*a_j^*a_i\cdot a_j$

Atom	x	y	z	U_{eq}/Å^2
Zr1	0.500	0.000	0.1723(5)	0.0284(4)
Cd1	0.000	0.000	0.9248(3)	0.067(1)
Cd2	0.000	0.000	0.4234(1)	0.0549(9)
O11	0.1218(7)	0.000	0.157(3)	0.049(3)
O31	0.000	0.1215(6)	0.679(3)	0.057(3)
O21	0.198(2)	0.000	0.486(3)	0.133(9)
O22	0.3848(9)	0.000	0.381(1)	0.046(3)
O41	0.000	0.197(2)	0.352(3)	0.10(1)
O12	0.3139(9)	0.000	0.093(2)	0.052(3)
O32	0.500	0.1864(9)	0.246(2)	0.052(3)
O42	0.500	0.114(1)	−0.038(2)	0.053(3)
OW1	0.196(2)	0.000	0.845(2)	0.090(8)
OW2	0.000	0.195(3)	0.995(3)	0.11(1)
OW3	0.500	0.000	0.714(2)	0.000(8)
OW4	0.246(3)	0.259(3)	0.119(7)	0.15(2)
C1	0.229(1)	0.000	0.189(3)	0.052(5)
C2	0.271(1)	0.000	0.365(2)	0.047(4)
C3	0.500	0.271(1)	0.154(5)	0.056(6)
C4	0.000	0.270(1)	0.477(2)	0.049(4)

alternating edge-shared $Cd1O_8$ and $Cd2O_8$ polyhedra. Each ZrO_8 polyhedron is linked to four $Cd2O_8$ polyhedra through a bidentate oxalate group leading to the three-dimensional framework. The resulting open framework exhibits tunnels with a square cross-section along [001] (edge dimension ~5 Å) (Fig. 5), as in $YK(C_2O_4)_2\cdot 4H_2O$,[1] and six-membered-ring tunnels along [111] (largest dimension ~6 Å) (Fig. 4), in which the water molecules not bonded to a cation (Ow3, Ow4) are located. Indeed, four of the water molecules participate in the cadmium coordination polyhedron and thus 2.3 water molecules in the compound must be considered as 'zeolitic'.

The cadmium and zirconium atoms both adopt the same type of environment, consisting of eight oxygen atoms forming a dodecahedron. The distances within these polyhedra, using the formalism introduced by Hoard and Silverton,[22] are reported in Table 3. The analysis of the distances using this notation permits one to show that both the zirconium and cadmium polyhedra are close to an ideal D_{2d} dodecahedron with six groups of distances M–A, M–B, *a*, *b*, *m* and *g* (see Fig. 6). Zirconium atoms are only surrounded by oxygen atoms from oxalate groups. The average distances 2.188 Å (M–A and M–B types), 2.565 Å (type *a*), 3.22 Å (type *b*), 2.555 Å (type *m*) and 2.695 Å (type *g*) in the ZrO_8 polyhedron are in good agreement with previously reported distances in compounds showing similar eight-fold coordinated Zr atoms, *e.g.* $Pb_2Zr(C_2O_4)_4\cdot nH_2O$[2] and $Zr(OH)_2(NO_3)_2\cdot 4.7H_2O$.[23] The environment of Cd2 also consists of eight oxygen atoms from four different oxalate groups with Cd2–O distances ranging from 2.28 Å (M–B type) to 2.64 Å (M–A type). The interatomic mean distances between oxygen atoms are 2.72 Å, 3.42 Å, 2.935 Å and 3.08 Å for *a*, *b*, *m* and *g* types, respectively. On the other hand, the Cd1 environment is made up of four oxygen atoms from two different oxalate groups and four oxygen atoms from water molecules. The shortest metal to oxygen distances within this polyhedron are found to be 2.27(2) Å (M–B type) with oxygen atoms from water molecules. The four longer distances, 2.49(3) Å (M–A type), are those between a cadmium atom and an oxygen atom belonging to an oxalate group. The inter-oxygen mean distances are 2.72 Å, 3.28 Å, 2.775 Å and 2.895 Å for *a*, *b*, *m* and *g*, respectively. The mean Cd–O distances within both cadmium dodecahedra, 2.36 Å for $Cd1O_8$ and 2.44 Å for $Cd2O_8$, are in good accordance with distances found in other compounds showing a similar dodecahedral arrangement, *e.g.* $K[C_3N_2H_5][Cd(C_2O_4)_2]$,[24] $Cd(NO_3)_2\cdot 4H_2O$[25] and $Cd_2(C_3H_2O_4)_2\cdot 4H_2O$.[26]

Table 3 Bond distances (Å) and angles (°) with their standard deviations for $Cd_2Zr(C_2O_4)_4\cdot 6.3H_2O$

Within the ZrO_8 polyhedra			
M–A		**M–B**	
Zr–O22^{I}	2.19(1)	Zr–O32	2.18(1)
Zr–O22	2.19(1)	Zr–O32^{I}	2.18(1)
Zr–O42	2.19(1)	Zr–O12	2.19(1)
Zr–O42^{I}	2.19(1)	Zr–O12^{I}	2.19(1)
a		***b***	
O22–O22^{I}	2.58(2)	O12–O32	3.22(1)
O42–O42^{I}	2.55(2)	O12^{I}–O32	3.22(1)
		O12–O32^{I}	3.22(1)
		O12^{I}–O32^{I}	3.22(1)
m		***g***	
O32–O42	2.55(2)	O12–O42	2.68(1)
O32^{I}–O42^{I}	2.55(2)	O42–O12^{I}	2.68(1)
O12–O22	2.56(2)	O12–O42^{I}	2.68(1)
O12^{I}–O22^{I}	2.56(2)	O12^{I}–O42^{I}	2.68(1)
		O22–O32	2.71(1)
		O22–O32^{I}	2.71(1)
		O22^{I}–O32	2.71(1)
		O22^{I}–O32^{I}	2.71(1)
Within the $Cd1O_8$ polyhedra			
M–A		**M–B**	
Cd1–O11^{III}	2.39(2)	Cd1–OW2	2.27(2)
Cd1–O11^{IV}	2.39(2)	Cd1–OW2^{II}	2.27(2)
Cd1–O31	2.49(2)	Cd1–OW1	2.30(2)
Cd1–O31^{II}	2.49(2)	Cd1–OW1^{II}	2.30(2)
a		***b***	
O31–O31^{II}	2.70(1)	OW1–OW2	3.28(2)
O11^{III}–O11^{IV}	2.74(2)	OW1–OW2^{II}	3.28(2)
		OW1^{II}–OW2^{II}	3.28(2)
		OW1^{II}–OW2	3.28(2)
m		***g***	
OW1–O11^{III}	2.78(3)	O11^{III}–OW2	2.87(2)
OW1^{II}–O11^{IV}	2.78(3)	O11^{III}–OW2^{II}	2.87(2)
OW2–O31	2.77(3)	O11^{IV}–OW2	2.87(2)
OW2^{II}–O31^{II}	2.77(3)	O11^{IV}–OW2^{II}	2.87(2)
		O31–OW1^{II}	2.92(3)
		O31^{II}–OW1^{II}	2.92(3)
		O31–OW1	2.92(3)
		O31^{II}–OW1	2.92(3)
Within the $Cd2O_8$ polyhedra			
M–A		**M–B**	
Cd2–O11	2.64(2)	Cd2–O21	2.28(2)
Cd2–O11^{II}	2.64(2)	Cd2–O21^{II}	2.28(2)
Cd2–O31	2.56(2)	Cd2–O41	2.29(2)
Cd2–O31^{II}	2.56(2)	Cd2–O41^{II}	2.29(2)
a		***b***	
O31–O31^{II}	2.70(1)	O21–O41	3.42(3)
O11–O11^{II}	2.74(2)	O21–O41^{II}	3.42(3)
		O41–O21^{II}	3.42(3)
		O41^{II}–O21^{II}	3.42(3)
m		***g***	
O11–O21	2.90(4)	O31–O21	3.07(2)
O11^{II}–O21^{II}	2.90(4)	O31–O21^{II}	3.07(2)
O41–O31	2.97(4)	O21–O31^{II}	3.07(2)
O41^{II}–O31^{II}	2.97(4)	O21^{II}–O31^{II}	3.07(2)
		O11^{II}–O41^{II}	3.09(2)
		O11–O41	3.09(2)
		O11^{II}–O41	3.09(2)
		O11–O41^{II}	3.09(2)
Within the oxalate groups			
C1–O11	1.23(2)	C3–O31^{VI}	1.22(2)
C1–O12	1.25(2)	C3–O32	1.23(3)
C2–O21^{a}	1.31(2)	C4–O41	1.34(3)
C2–O22^{a}	1.29(2)	C4–O42^{V}	1.31(2)
C1–C2^{a}	1.56(2)	C3–C4^{V}	1.57(5)
O11–C1–O12	127(2)	O31^{V}–C3–O32	131(4)
O21–C2–O22	123(2)	O41–C4–O42^{VI}	122(2)
O11–C1–C2	120(2)	O31–C3–C4^{V}	117(3)
O12–C1–C2	113(1)	O32–C3–C4^{V}	112(2)
O21–C2–C1	124(2)	O41–C4–C3^{VI}	125(2)
O22–C2–C1	113(1)	O42^{VI}–C4–C3^{VI}	113(2)

Symmetry code: I, $1-x$, $-y$, z; II, $-x$, $-y$, z; III, x, y, $1+z$; IV, $-x$, $-y$, $1+z$; V, $\frac{1}{2}-x$, $\frac{1}{2}-y$, $\frac{1}{2}-z$; VI, $\frac{1}{2}-x$, $\frac{1}{2}-y$, $z-\frac{1}{2}$. [a]Constrained.

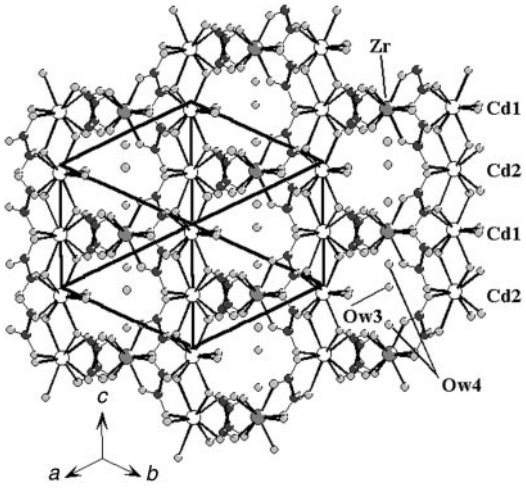

Fig. 4 Projection of the structure of $Cd_2Zr(C_2O_4)_4{\cdot}6.3H_2O$ along [111]. Large white circles: Cd; large grey circles: Zr; small black circles: C; small grey circles: O and H_2O.

The structure possesses two different oxalate groups which are strictly planar because all of the oxygen and carbon atoms lie on mirror planes. The two crystallographically different oxalates are also perpendicular to one another since they belong to a different mirror plane. Within the partially constrained oxalate group, the carbon to oxygen distances are 1.23(2) Å and 1.25(2) Å for C1–O11 and C1–O12, respectively. The bond distances and angles within the second oxalate group [mean distances: C–O 1.27 Å, C3–C4 1.57 Å; mean angles: O–C–O 127°, O–C–C 117°] agree well with the mean values 1.24 Å, 1.55 Å, 125° and 117°, respectively, reported by Hahn[27] for oxalate compounds.

Possible hydrogen bonds were located in accordance with Baur and Khan's criteria,[28] *i.e.* "the oxygen–oxygen distance has to be smaller than 3.1 Å, the two oxygen atoms must not belong to the same coordination polyhedron and the bond angle O(acceptor)–Ow–O(acceptor) should not deviate more than 35° from the tetrahedral angle". Possible hydrogen bonds are found between water molecules lying in the channels together, on one hand, and between a water molecule and an oxygen atom belonging to the cadmium environment, on the other. It can be thought that these bonds are fairly weak because of the easiness for those water molecules to leave the structure. These results are displayed in Fig. 7 and the corresponding bond lengths and angles are reported in Table 4.

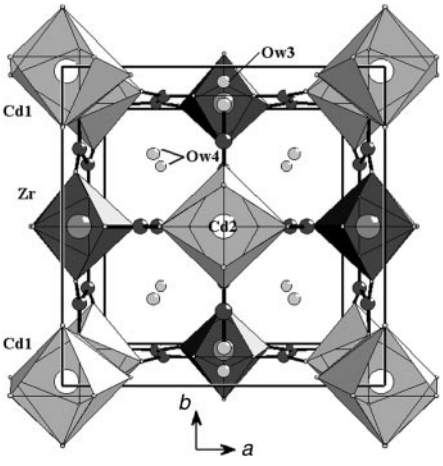

Fig. 5 Perspective view of the structure of $Cd_2Zr(C_2O_4)_4{\cdot}6.3H_2O$ along [001]. Large white circles: Cd; large grey circles: Zr; small black circles: C; small grey circles: O and H_2O.

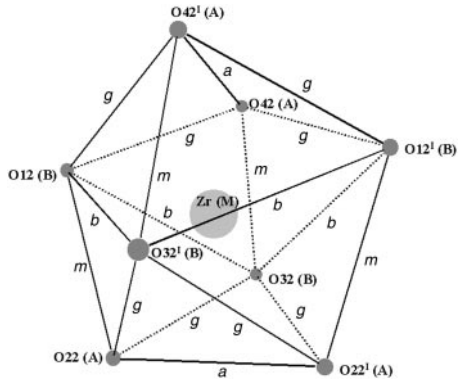

Fig. 6 Coordination polyhedron of the zirconium atom. The O···O distances are indicated according to the common notation used by Hoard and Silverton.[22]

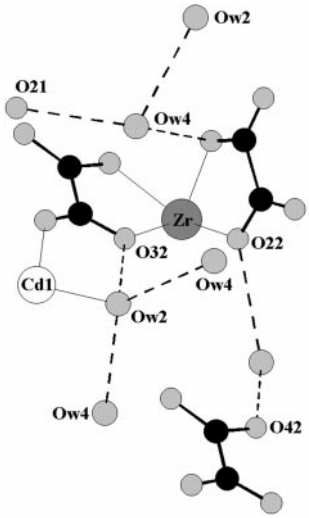

Fig. 7 Environment of the 'zeolitic' water molecules in $Cd_2Zr(C_2O_4)_4{\cdot}6.3H_2O$. The possible hydrogen bonds are represented by dotted lines. Large white circles: Cd; large grey circles: Zr; small black circles: C; small grey circles: O and H_2O.

Thermal decomposition

Figs. 8 and 9 display the TG curve and the three-dimensional representation of the successive X-ray powder diffraction patterns recorded during the decomposition of the precursor under dynamic air. Three main stages for the decomposition of the precursor can be deduced from the TG curve, instead of apparently two from the TDXD study. From the TG measurements, the chemical formula of the precursor sample used was found to be $Cd_2Zr(C_2O_4)_4{\cdot}7.5H_2O$ at room temperature. It is slightly different from $Cd_2Zr(C_2O_4)_4{\cdot}6.3H_2O$ as found from the structure determination. This discrepancy

Table 4 Possible hydrogen bond lengths (Å) and angles (°) with their estimated standard deviations for $Cd_2Zr(C_2O_4)_4{\cdot}6.3H_2O$.

Ow2–Ow4^{III}	3.03(4)	O32^{IX}–Ow2–Ow4^{III}	100(1)
Ow2–Ow4^{VIII}	3.03(4)	O32^{IX}–Ow2 –Ow4^{IX}	100(1)
Ow2–O32^{IX}	2.49(3)	Ow4^{III}–Ow2–Ow4^{IX}	130(2)
Ow3–O22^{I}	3.11(2)	O22^{I}–Ow3–O42^{III}	141.0(2)
Ow3–O42^{III}	2.45(2)		
Ow4–O12	3.01(3)	O12–Ow4–Ow2^{VII}	89(1)
Ow4–O21^{VI}	2.99(4)	O21^{VI}–Ow4–Ow2^{VII}	106(1)
Ow4–Ow2^{VII}	3.03(4)	O12–Ow4–O21^{VI}	142(2)
Ow4–O32	3.15(4)	O32–Ow4–O21^{VI}	99.9(9)

Symmetry codes: I, $1-x$, $-y$, z; III, x, y, $1+z$; VI, $\frac{1}{2}-x$, $\frac{1}{2}-y$, $z-\frac{1}{2}$; VII, x, y, $z-1$; VIII, $-x$, y, $1+z$; IX, $\frac{1}{2}-x$, $\frac{1}{2}-y$, $\frac{1}{2}+z$.

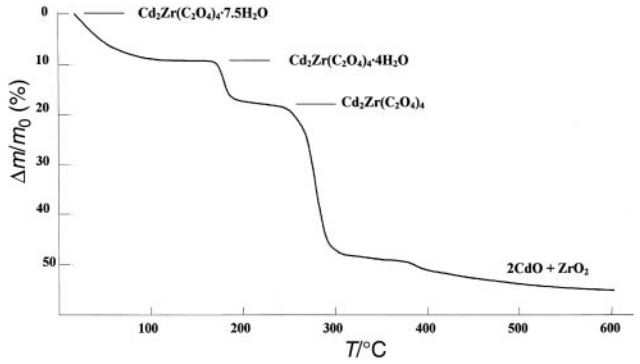

Fig. 8 TG curve for $Cd_2Zr(C_2O_4)_4{\cdot}7.5H_2O$ under air (5 °C h^{-1} between 18 and 400 °C, then 25 °C h^{-1} up to 600 °C).

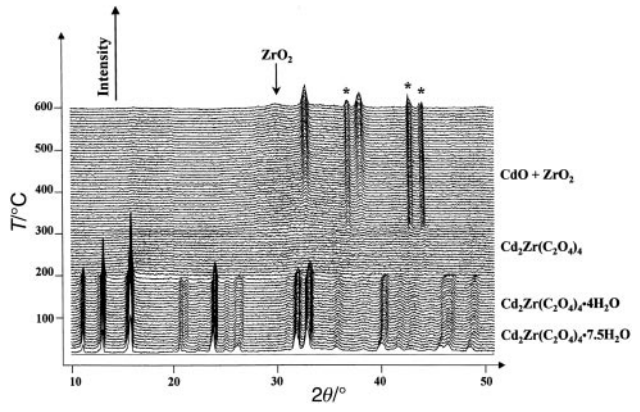

Fig. 9 TDXD plot for $Cd_2Zr(C_2O_4)_4{\cdot}7.5H_2O$ under air (15 °C h^{-1} in the range 18-600 °C, counting time 1800 s per pattern); * diffraction lines from the sample holder.

demonstrates the sensitivity of the water content to ambient atmosphere conditions. The TG curve clearly shows that the two first stages, in the temperature ranges 20–150 °C and 150–230 °C, consist of two successive dehydration processes with the loss of 3.5 H_2O (~8.7%) and 4 H_2O (~9.3%), respectively, and lead to the successive phases $Cd_2Zr(C_2O_4)_4{\cdot}4H_2O$ and $Cd_2Zr(C_2O_4)_4$. From the TDXD plot (Fig. 9), it can be seen that the successive diffraction patterns are very similar in the temperature range 20–180 °C, though some X-ray diffraction lines shift slightly between 20 and 80 °C. This is in agreement with the results reported in the powder diffraction study on the temperature dependence of the parameters of the orthorhombic lattice (Fig. 3). Consequently, these results give evidence that the initial structure is preserved during the first stage of the dehydration and that the shift of some diffraction lines is correlated to the decrease of the cell parameters during the progressive dehydration. This feature and the sensitivity of the water content in the precursor towards the ambient conditions deserve to be thoroughly described. For clarity, the chemical formula of the precursor is reflected in the formula $Cd_2Zr(C_2O_4)_4{\cdot}(4+n)H_2O$.

Initial stage of dehydration. To characterise the initial dehydration process, experiments were carried out under selected water vapour pressures. Fig. 10 displays the variation of the number of water molecules exceeding four, *i.e. n versus* time. These values were obtained from the TG curve recorded under $P(H_2O) = 10$ Torr with temperature stages scanned every 5 °C within the range 20–60 °C. Fig. 10 shows that n equals 3.62 at 21 °C. This decreases to 0.55 when the temperature reaches 60 °C, but stays constant for each selected temperature stage. Furthermore, an immediate decrease of n is observed as soon as the temperature increases. This feature indicates that a

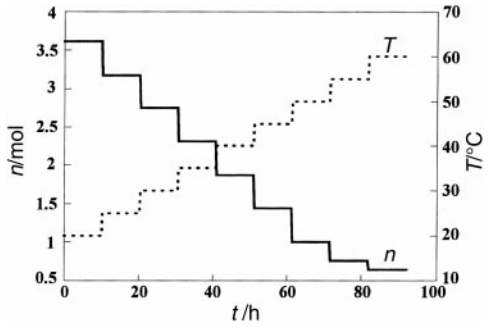

Fig. 10 Variations of the water content n during the dehydration of $Cd_2Zr(C_2O_4)_4{\cdot}(4+n)H_2O$ under a water vapour pressure $P(H_2O) =$ 10 Torr ($n = 3.62$), showing that n is constant at a given temperature.

thermodynamical equilibrium is immediately reached for each temperature. In addition, complementary experiments have shown that this reaction is totally reversible upon cooling. Consequently, it can be concluded that the water content exceeding four inside the material depends on both the water vapour pressure and the temperature, according to a divariant system. The corresponding water molecules can then be considered as truly 'zeolitic' water. These water molecules are clearly those that are non-bonded to a cation and located inside the tunnels of the structure with a square cross-section running along [001] (Fig. 5) and with an ellipsoidal cross section running along [111] (Fig. 4). There is no change in the structure framework due to the departure of these molecules from the channels, even though there is a significant decrease of the cell parameters (Fig. 3).

Several TG experiments were carried out under selected water vapour pressures $P(H_2O)$. As the thermodynamical equilibrium between two successive hydrated phases is immediately reached for a given temperature as seen above, the evolution of the water content n as a function of temperature could be easily determined from the TG curves performed at selected $P(H_2O)$ with a slow heating rate of 3 °C h^{-1}. The plots displayed in Fig. 11 summarise these results.

It can be seen that n decreases linearly with temperature down to about 1, for $P(H_2O) > 6.05$ Torr. On the other hand, the total elimination of the 'zeolitic' water molecules from the channels requires heating the sample at temperatures > 110 °C, depending upon the water vapour pressure imposed. From these plots, it was possible to determine the equilibrium parameters $P(H_2O)$–T for a given value n. Fig. 12 shows that $P(H_2O)$ fits the general relationship, for n in the range 1–3.5, given by eqn. (1):

$$\ln P(H_2O) = (A/T) + B \quad (1)$$

Eqn. (1) is derived from the standard free enthalpy of the following dehydration reaction

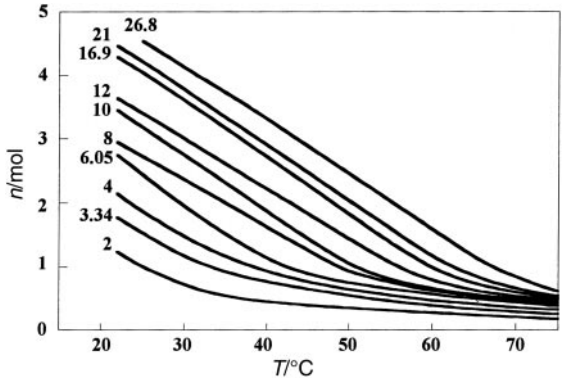

Fig. 11 Water content n as a function of temperature for selected water vapour pressures $P(H_2O)$ in the range 2–27 Torr.

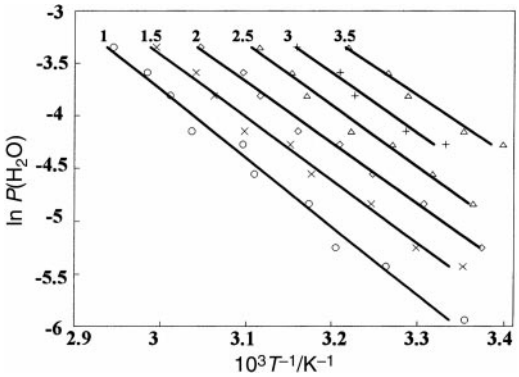

Fig. 12 Plot of ln $P(H_2O)$ *versus* T^{-1} for various water contents n in $Cd_2Zr(C_2O_4)_4{\cdot}(4+n)H_2O$.

$$Cd_2Zr(C_2O_4)_4{\cdot}(4+n)H_2O_{(cr)} \rightarrow$$
$$Cd_2Zr(C_2O_4)_4{\cdot}[4+(n-1)]H_2O_{(cr)} + H_2O_{(g)}$$

for which the equilibrium constant is $P(H_2O)/P^\circ$, where P° is the standard pressure. The enthalpy, Δ_rH, and the entropy, Δ_rS, of this reaction were calculated for different values of n from the slope A ($\Delta_rH = -RA$) and the intercept B ($\Delta_rS = RB$), where R is the gas constant. The results are summarised in Table 5. It can be considered that Δ_rH and Δ_rS are independent of n. The mean value 49(2) kJ mol^{-1} for Δ_rH can be compared with the commonly accepted sublimation enthalpy of solid water (52.1 kJ mol^{-1}) or with the mean energy of two hydrogen bonds ($\sim$50 kJ). The mean value of Δ_rH is less than the values observed for the dehydration of $Pb_2Zr(C_2O_4)_4{\cdot}nH_2O$[2] (mean value $\sim$57 kJ mol^{-1}) and $YK(C_2O_4)_2{\cdot}4H_2O$[1] (values in the range 54.2–70.2 kJ mol^{-1}), where the water molecules are bonded to either a lead or a potassium atom. This comparison confirms that the water molecules located inside the channels of the structure of $Cd_2Zr(C_2O_4)_4{\cdot}(4+n)H_2O_{(cr)}$ are purely 'zeolitic' and suggests that the hydrogen bond strengths involving these water molecules are similar to those occurring in solid water.

Second stage of dehydration and decomposition. The dehydration of $Cd_2Zr(C_2O_4)_4{\cdot}4H_2O$ takes place from temperatures that depend on the water vapour pressure in the reactor. From TG measurements performed under different water vapour pressures the onset temperatures of the dehydration can be determined as a function of $P(H_2O)$. The enthalpy and the entropy of dehydration were calculated as described above and were found to be 80(1) kJ mol^{-1} and 141(2) J K^{-1} mol^{-1}, respectively. These values are greater than those found for the departure of 'zeolitic' water molecules and provide evidence that the four water molecules involved in the second dehydration process are strongly bonded in the precursor structure. Indeed, these water molecules participate in the coordination polyhedron $Cd1O_8$. Their departure leads to the total destruction of the structure framework and yields an anhydrous phase amorphous to X-rays (Fig. 9). The last stage of the decomposition occurs from about 240 °C as shown from the TG curve (Fig. 8) [$P(H_2O) \approx 10$ Torr]. The weight loss is rapid between 240 and 300 °C and slower from 300 to 600 °C, where the total weight loss reaches 53.8% (theoretical weight loss 54.7%, calculated for the formation of a solid with the global chemical formula Cd_2ZrO_4). The TDXD plot (Fig. 9) shows the X-ray diffraction lines of CdO that emerge from the background from 300 °C and a very broad line situated at 30.2° (2θ) beyond 500 °C corresponding to the strongest line of cubic ZrO_2. Consequently, it can be concluded that the anhydrous phase $Cd_2Zr(C_2O_4)_4$ decomposes into a mixture of two phases, namely CdO and nanocrystalline ZrO_2. The formation of nanocrystalline ZrO_2 in the thermal decomposition of inorganic precursors with low thermal stability has already been reported, *e.g.* in the study of the thermal behaviour of zirconium hydroxide nitrates.[29,30] Nevertheless, for the latter compounds it was proved that the crystallisation of amorphous ZrO_2 with increasing temperatures led to the tetragonal variety of ZrO_2, while in the present study cubic ZrO_2 is surprisingly formed. The formation of cubic ZrO_2 [$a = 5.122(3)$ Å] was demonstrated by heating the oxide mixture (CdO, ZrO_2) at 800 °C for 1 h and then quenching to room temperature. It should be noted that the stabilisation of the cubic variety has already been reported for Cd-doped ZrO_2 in the CdO–ZrO_2 system.[31]

Table 5 Enthalpy Δ_rH and entropy Δ_rS of dehydration as a function of the number n of 'zeolitic' water molecules

n/mol	Δ_rH/kJ mol^{-1}	Δ_rS/J K^{-1} mol^{-1}
1.0	53(1)	128(5)
1.5	49(1)	119(4)
2.0	48(1)	119(4)
2.5	48(2)	121(6)
3.0	49(3)	126(8)
3.5	47(2)	123(7)

Conclusion

The present study shows that, in spite of serious instability problems, the crystal structure of $Cd_2Zr(C_2O_4)_4{\cdot}(4+n)H_2O$ has been satisfactorily determined and the thermodynamical investigation has contributed to explain the dynamic behaviour of the material. Due to the flexibility of the cadmium polyhedron, cadmium can both adopt an eight-fold coordination and combine with eight-fold coordinated zirconium atoms to form the new cadmium zirconium oxalate $Cd_2Zr(C_2O_4)_4{\cdot}(4+n)H_2O$. It is of note that the crystal structure has the structure-type of $YK(C_2O_4)_2{\cdot}4H_2O$, even though the crystal symmetry and metal valences are different. This structure type explains the interesting zeolitic properties reported for these compounds, as well as the reversible 'elastic' properties of the structure framework upon initial dehydration and hydration. The results described here show that the structure building concept based on eight-fold coordinated metals can further be exploited for the synthesis of new oxalate materials with open crystal structures and related dynamic properties. Some recent studies relating to this area confirm the possibility to extend this idea to new materials.

Acknowledgements

Dr T. Roisnel and Mr G. Marsolier are acknowledged for their technical assistance in single-crystal and powder diffraction data collection.

References

1 T. Bataille, J. P. Auffrédic and D. Louër, *Chem. Mater.*, 1999, **11**, 1559.
2 C. Boudaren, J. P. Auffrédic, M. Louër and D. Louër, *Chem. Mater.*, 2000, **12**, 2324.
3 C. Sterling, *Nature*, 1965, **205**, 588.
4 N. Gérard, G. Watelle-Marion and A. Thrierr-Sorel, *Bull. Soc. Chim. Fr.*, 1968, **11**, 4367.
5 E. Hanson, *Acta Chem. Scand.*, 1970, **24**, 2969.
6 O. Chaix-Pluchery, J. C. Mutin, J. Bouillot and J. C. Niepce, *Acta Crystallogr., Sect. C*, 1989, **45**, 1699.
7 G. Férey, *J. Solid State Chem.*, 2000, **152**, 37.
8 P. Bénard-Rocherullé, J. Rius and D. Louër, *J. Solid State Chem.*, 1997, **128**, 295.
9 D. Louër and J. I. Langford, *J. Appl. Crystallogr.*, 1988, **21**, 430.
10 A. Boultif and D. Louër, *J. Appl. Crystallogr.*, 1991, **24**, 987.
11 J. Rodriguez-Carvajal, in *Collected Abstracts of Powder Diffraction Meeting*, Toulouse, France, 1990, pp. 127–128.

12 J. Rodriguez-Carvajal and T. Roisnel, in *Newsletter*, Commission on Powder Diffraction, International Union of Crystallography, Chester, 1998, vol. 20, p. 35.
13 J. Plévert, J. P. Auffrédic, M. Louër and D. Louër, *J. Mater. Sci.*, 1989, **24**, 1913.
14 Nonius, Kappa CCD Program Software, Nonius BV, Delft, The Netherlands, 1998.
15 Z. Otwinowski and W. Minor, *Methods Enzymol.*, 1997, **276**, 307.
16 P. Coppens, *Crystallographic Computing*, ed. F. R. Ahmed, S. R. Hall and C. P. Huber, Munksgaard Publishers, Copenhagen, 1970, pp. 255–270.
17 M. Boll, *Mémento du Chimiste*, Dunod, Paris, 1949.
18 International Centre for Diffraction Data, Newtown Square, PA.
19 A. Altomare, M. C. Burla, M. Camalli, G. Cascarano, C. Giacovazzo, A. Guagliardi, A. G. G. Moliterni, G. Polidori and R. Spagna, *J. Appl. Crystallogr.*, 1999, **32**, 115.
20 G. M. Sheldrick, *Acta Crystallogr., Sect. A*, 1990, **46**, 467.
21 G. M. Sheldrick, *SHELXL-97: Programs for Crystal Structure Refinement*, University of Göttingen, Göttingen, 1997.
22 J. L. Hoard and J. V. Silverton, *Inorg. Chem.*, 1963, **2**, 235.
23 P. Bénard, M. Louër and D. Louër, *J. Solid State Chem*, 1991, **94**, 27.
24 A. Prasad, S. Neeraj, S. Natarajan and C. N. R. Rao, *Chem. Commun.*, 2000, 1251.
25 B. Matković, B. Ribar and B. Zelenko, *Acta Crystallogr.*, 1966, **21**, 719.
26 K. H. Chung, E. Hong, Y. Do and C. H. Moon, *J. Chem. Soc., Chem. Commun.*, 1995, 2333.
27 T. Hahn, *Z. Anorg. Allg. Chem.*, 1957, **109**, 438.
28 W. H. Baur and A. A. Khan, *Acta Crystallogr., Sect. B*, 1970, **26**, 1584.
29 P. Bénard, J. P. Auffrédic and D. Louër, *Powder Diffr.*, 1993, **8**, 39.
30 P. Bénard and D. Louër, *J. Phys. Chem. Solids*, 1995, **56**, 1345.
31 S. N. Sapon, V. B. Nalbandyan, I. N. Belyaev and S. S. Lopatin, *Russ. J. Inorg. Chem.*, 1982, **27**, 903.